



# HOKKAIDO UNIVERSITY

Title	AN S-WAVE MULTIPLE-SCATTERING APPROACH TO LOW-ENERGY ELECTRON DIFFRACTION BY CRYSTAL SURFACES
Author(s)	HAMAUZU, Yoshihiro
Citation	JOURNAL OF THE RESEARCH INSTITUTE FOR CATALYSIS HOKKAIDO UNIVERSITY, 23(2), 79-90
Issue Date	1976-03
Doc URL	<a href="https://hdl.handle.net/2115/24990">https://hdl.handle.net/2115/24990</a>
Type	departmental bulletin paper
File Information	23(2)_P79-90.pdf



## AN S-WAVE MULTIPLE-SCATTERING APPROACH TO LOW-ENERGY ELECTRON DIFFRACTION BY CRYSTAL SURFACES<sup>\*</sup>)

By

Yoshihiro HAMAUZU<sup>\*\*)</sup>

(Received January 8, 1974)

### Abstract

A method for calculating low-energy electron diffraction (LEED) intensities is developed on the basis of the s-wave approximation. The intensities of LEED spots are calculated by using the value of the wavefunction at the atomic center in a crystal, which is determined by a set of simultaneous linear equations.

The LEED intensities of the (00), {10}, and {11} beams from the copper (100) surface have been calculated in the energy range 0-100 eV. The primary Bragg peaks in the calculated LEED intensities are in good agreement with experiments, whereas the heights of the secondary Bragg peaks are too small as compared with experiments.

It has been found that the distance between the first and second atomic layers of the Cu (100) surface neither relax nor contract more than 10% of the bulk value.

### § 1. Introduction

It is one of the most important problems in surface science to know surface structure of solids. The structure of solid surfaces can be determined by analyzing both the patterns (spots) of low-energy electron diffraction (LEED) and their intensities. The analysis of LEED patterns has revealed many interesting and sometimes surprising features of crystal surfaces<sup>1)</sup>, and contributed very much to the development of surface science.

It is to be noted that we can determine only the structure of unit nets of crystal surfaces by analyzing LEED patterns. In other words, if we wish to know the details of the three-dimensional structure of crystal surfaces, we have to analyze LEED spectra, *i. e.*, intensity-energy curve for the diffracted beams<sup>2)</sup>. Unfortunately the simple kinematical theory taking

---

<sup>\*</sup>) A part of this paper was presented at the Ninth International Congress of Crystallography held in Kyoto, Japan (1972), the abstract of the talk being published in *Acta Cryst.*, **A 28** (S 4), 228 (1972).

<sup>\*\*)</sup> Research Institute for Catalysis, Hokkaido University, Sapporo, Japan.

account only of the single scattering events is not adequate for analyzing LEED spectra, so that a dynamical theory has to be used instead. Several dynamical theories of LEED have been developed. In order to calculate LEED spectra by using these theories, we have to solve a set of simultaneous linear equations (the self-consistent multiple scattering theory<sup>3~5)</sup> or a matrix eigenvalue problem (the band structure matching method<sup>6~9)</sup> and the layer-by-layer method<sup>10,11)</sup>, both of large dimensions, which requires a lot of computing time. This has made surface structure determination from LEED spectra very difficult. Hence it is desirable to develop an approximation method which does not require too much computing time.

It is the purpose of the present paper to develop a simplified method for calculating LEED spectra. This method is based on the s-wave approximation, in which the scattering of electrons by an atom is assumed isotropic. DUKE and TUCKER<sup>12)</sup>, and HIRABAYASHI<sup>13)</sup> also used the s-wave approximation in their theories of LEED. In the present method the LEED spectra for a given crystal are calculated by using the values of the wavefunctions at the atomic centers in the crystal, which are determined by a set of simultaneous linear equations.

To test the validity of the present method LEED spectra from the copper (100) surface are calculated and compared with experiments.

## § 2. Method

Let us proceed with the following basic assumptions. (1) The crystal has a two-dimensional translational symmetry. (2) The primary wave is a plane wave. (3) The amplitude of the scattered wave by an atom is isotropic. (4) The effects of the inelastic scattering processes on the elastic waves are taken into account by using a uniform imaginary potential. (5) The scattering of an incident electron by a surface potential barrier is neglected.

Then the Schrödinger equation describing the diffraction processes are :  
in a vacuum,

$$-\nabla^2 \Psi(\boldsymbol{r}) = E \Psi(\boldsymbol{r}), \quad (1)$$

and in a crystal,

$$\left(-\nabla^2 + V(\boldsymbol{r}) - V_0\right) \Psi(\boldsymbol{r}) = E \Psi(\boldsymbol{r}). \quad (2)$$

Here  $V_0$  and  $E$  denote the inner potential and the energy of the incident electron, respectively. According to assumption (4), we can put<sup>14)</sup>

*An S-Wave Multiple-Scattering Approach to Low-Energy Electron Diffraction*

$$V_0 = V_0^r + iV_0^i$$

The Schrödinger Eq. (2) is transformed to an integral equation,

$$\Psi(\mathbf{r}) = e^{iKz} + \int_{\text{crystal}} \mathcal{G}_0(\mathbf{r}-\mathbf{r}') V(\mathbf{r}') \Psi(\mathbf{r}') d\mathbf{r}', \quad (3)$$

where

$$K^2 = E + V_0^r + iV_0^i, \quad (4)$$

and

$$\mathcal{G}_0(\mathbf{r}-\mathbf{r}') = -\frac{1}{4\pi} \frac{e^{iK|\mathbf{r}-\mathbf{r}'|}}{|\mathbf{r}-\mathbf{r}'|}. \quad (5)$$

In Eq. (3) the integration is to be carried out over the whole crystal. Let the  $x$ - $y$  plane be the parallel to the crystal surface plane and let  $\mathbf{a}_1$  and  $\mathbf{a}_2$  be the primitive translation vectors in the  $x$ - $y$  plane; then the crystal is divided into the "reference columns"<sup>15)</sup>, each with the unit net as its basal plane (Fig. 1). Now the potential function  $V(\mathbf{r})$  is expressed as the sum of the contributions from the reference columns, *i. e.*,

$$V(\mathbf{r}) = \sum_{\mathbf{q}} V_{\text{R.C.}}(\mathbf{r}-\mathbf{q}), \quad (6)$$

with

$$\mathbf{q} = q_1 \mathbf{a}_1 + q_2 \mathbf{a}_2 \quad (7)$$

where  $\mathbf{q}$  is a lattice vector in two dimensions.

Substitution of Eq. (6) into Eq. (3) gives

$$\Psi(\mathbf{r}) = e^{iKz} + \int_{\text{R.C.}} G_{\text{st}}(\mathbf{r}-\mathbf{r}') V_{\text{R.C.}}(\mathbf{r}') \Psi(\mathbf{r}') d\mathbf{r}', \quad (8)$$

where

$$G_{\text{st}}(\mathbf{r}-\mathbf{r}') = \sum_{\mathbf{q}} \mathcal{G}_0(\mathbf{r}-\mathbf{r}'-\mathbf{q}) e^{iK_1 \cdot \mathbf{q}}. \quad (9)$$

Here  $G_{\text{st}}(\mathbf{r}-\mathbf{r}')$  is called the structural Green's function and  $K$  is the surface component of the propagation vector of the incident electron. In the case of  $z \neq z'$ , the Green's function (9) is expressed as the summation over the reciprocal vectors<sup>16)</sup>,

$$G_{\text{st}}(\mathbf{r}-\mathbf{r}') = \sum_{\mathbf{v}} \frac{1}{2iAK_{\mathbf{v}}} e^{iK_{\mathbf{v}}^{\pm}(\mathbf{r}-\mathbf{r}')}, \quad (10)$$

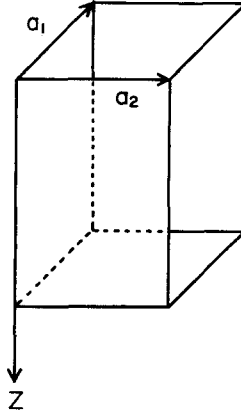


**Fig. 1.** Reference column;  $\mathbf{a}_1$  and  $\mathbf{a}_2$  are primitive translation vectors and the  $z$ -axis is normal to the surface.

where  $A$  is the area of a unit net and  $\mathbf{v}$  is a reciprocal vector, *i. e.*

$$\begin{aligned} \mathbf{v} &= 2\pi(\nu_1 \mathbf{b}_1 + \nu_2 \mathbf{b}_2), \\ \mathbf{a}_i \mathbf{b}_j &= \delta_{ij} \quad (i, j=1, 2), \end{aligned} \quad (11)$$

and  $\mathbf{K}_{\mp}^{\dagger}$  denotes the propagation vector, *i. e.*

$$\mathbf{K}_{\mp}^{\dagger} = (\mathbf{K}_{11} + \mathbf{v}, \pm K_{\nu}), \quad (12)$$

$$K_{\nu} = [E + V_0 + iV_0' - (\mathbf{K}_{11} + \mathbf{v})^2]^{1/2}. \quad (13)$$

In Eq. (10) the plus and minus signs correspond to the cases  $z > z'$  and  $z < z'$ , respectively.

### 2.1 Amplitude reflection coefficient

The amplitude reflection coefficient  $C_{\nu}$  appropriate to the reciprocal vector  $\mathbf{v}$  is given by using Eqs. (8) and (10) as

$$C_{\nu} = (1/2 iAK_{\nu}) \int_{\text{R.C.}} e^{-i\mathbf{K}_{\nu}^{\dagger} \mathbf{r}'} V_{\text{R.C.}}(\mathbf{r}') \Psi(\mathbf{r}') d\mathbf{r}'. \quad (14)$$

Let  $V_{\mu i}(\mathbf{r})$  denote the potential function of the atom  $(\mu, i)$  which belongs to the unit net at the  $\mu$ -th atom layer in the reference column. Then we may write

$$V_{\text{R.C.}}(\mathbf{r}) = \sum_{\mu i} V_{\mu i}(\mathbf{r} - \mathbf{R}_{\mu i}), \quad (15)$$

where  $\mathbf{R}_{\mu i}$  is the position vector of the atom  $(\mu, i)$ . According to assumption (3), we can replace the potential  $V_{\mu i}(\mathbf{r})$  by the Fermi pseudopotential<sup>17)</sup>;

$$V_{\mu i}(\mathbf{r}) = -4\pi \mathcal{A}_{\mu i}(K) \delta(\mathbf{r}), \quad (16)$$

with

$$\mathcal{A}_{\mu i}(K) = (e^{2i\delta_{\mu i}(K)} - 1)/2iK \quad (17)$$

Here  $\delta_{\mu i}(K)$  is the  $s$ -wave phase shift of an electron scattered by the atom  $(\mu, i)$ . With the help of Eqs. (15) and (16), the amplitude reflection coefficient  $C_{\nu}$  is expressed as

$$C_{\nu} = (2\pi i/AK_{\nu}) \sum_{\mu i} e^{-i\mathbf{K}_{\nu}^{\dagger} \mathbf{R}_{\mu i}} \mathcal{A}_{\mu i}(K) \Psi(\mathbf{R}_{\mu i}). \quad (18)$$

Here  $\Psi(\mathbf{R}_{\mu i})$  is the value of the wavefunction at the center of the atom  $(\mu, i)$ . If we can determine the value of  $\Psi(\mathbf{R}_{\mu i})$ , the amplitude reflection coefficient  $C_{\nu}$  is calculated from Eq. (18). It is to be remembered that the intensity of the diffracted beams corresponding to the reciprocal vector  $\mathbf{v}$  is proportional to  $|C_{\nu}|^2$ .

*An S-Wave Multiple-Scattering Approach to Low-Energy Electron Diffraction*

## 2.2 Wavefunction

We shall derive equations for determining  $\Psi(R_{\mu i})$ . For this purpose, we carry out the integration with respect to  $\mathbf{r}'$  in Eq. (8) with the help of Eqs. (15) and (16), and we obtain

$$\Psi(\mathbf{r}) = e^{iK\mathbf{r}} + \sum_{\mu i} G_{st}(\mathbf{r}-R_{\mu i})(-4\pi) \mathcal{A}_{\mu i}(K) \Psi(R_{\mu i}). \quad (19)$$

By putting  $\mathbf{r} = \mathbf{R}_{\nu j}$ , Eq. (19) becomes a set of simultaneous linear equations for the unknown;

$$\begin{aligned} \Psi(R_{\nu j}) &= e^{iK R_{\nu j}} + G(0) \mathcal{A}_{\nu j}(K) \Psi(R_{\nu j}) \\ &+ \sum_{i(\neq j)} G_{\nu j, \nu i} \mathcal{A}_{\nu i}(K) \Psi(R_{\nu i}) \\ &+ \sum_{\mu i(\mu \neq \nu)} G_{\nu j, \mu i} \mathcal{A}_{\mu i}(K) \Psi(R_{\mu i}), \end{aligned} \quad (20)$$

where

$$G_{\nu j, \mu i} = -4\pi \sum_{\mathbf{q}} \mathcal{G}_0(R_{\nu j} - R_{\mu i} - \mathbf{q}) e^{iK_{11}\mathbf{q}}, \quad (21)$$

and

$$G(0) = \sum_{\mathbf{q} \neq 0} \frac{e^{iK\mathbf{q}}}{|\mathbf{q}|} e^{iK_{11}\mathbf{q}}. \quad (22)$$

In the case of  $z_{\mu} \neq z_{\nu}$  it is convenient to use Eq. (23) below, rather than Eq. (21), as the Green's function;

$$G_{\nu j, \mu i} = \sum_{\mathbf{p}} (2\pi i / AK_{\mathbf{p}}) e^{iK_{\mathbf{p}}^{\pm}(R_{\nu j} - R_{\mu i})}. \quad (23)$$

It is to be noted that the summation over lattice vector in Eq. (22) is absolutely convergent because  $K$  is complex according to Eq. (4).

### § 3. LEED spectra from the copper (100) surface

First we describe the nature of the parameters in the Eqs. (20), (21), and (23). Since the real part of the inner potential is the space-averaged scattering potential, it is approximately equal to the work function  $\zeta$  plus the Fermi energy  $E_F$  measured from the muffin-tin zero. In the case of copper,  $E_F$  is 7.7 eV and  $\zeta$  is 4.5 eV, so that  $V_0 = 12.2$  eV<sup>(18)</sup>. On the other hand, the value  $V_0$  can be determined by comparing the calculated LEED spectra with experimental ones<sup>(19)</sup>. In the present calculation we obtain  $V_0 = 13$  eV, which is in good agreement with the value mentioned above. Here we adopt the latter value as the inner potential because it includes the dynamical effects between electrons.

The imaginary part of the inner potential is connected with the electron mean free path  $\lambda_{ee}$  according to the uniform damping model<sup>12)</sup>:

$$V_0^i = 2\sqrt{E + V_0^r}/\lambda_{ee}. \quad (24)$$

We treat both the electron mean free path and the  $s$ -wave phase shift as empirical parameters.

An incident electron penetrates into only a few atom layers because both of the strong absorption and large atomic scattering factors. The LEED spectra from the copper (100) surface with seven atom layers (Fig. 2) have shown good convergence. In Fig. 2 the Cartesian axes are indicated. The polar and azimuthal angles will be denoted by  $\theta$  and  $\phi$  in Figs. 3-9, respectively.

### 3.1 Electron mean free path and LEED spectra

Figure 3 shows LEED spectra of the (00) beam calculated by using three values indicated in the figure caption for  $\lambda_{ee}$ . Other parameters used are indicated in the panel. The peak near 35 eV is a primary Bragg peak caused by a single scattering

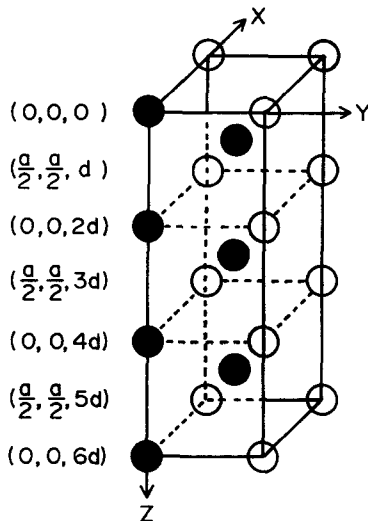


Fig. 2. Reference column with seven atomic layers for the copper (100) surface. The Cartesian coordinates of black circles are indicated on the left side of the reference column, where  $a$  and  $d$  are 2.56 Å and 1.86 Å, respectively.

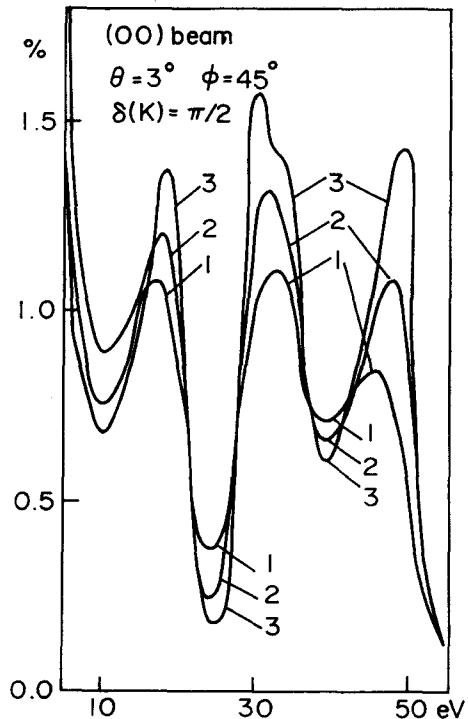


Fig. 3. Dependence of LEED spectra on the electron mean free path.  $\lambda_{ee}$ : 1) 6 Å, 2) 8 Å, 3) 10 Å.

*An S-Wave Multiple-Scattering Approach to Low-Energy Electron Diffraction*

and other peaks in the spectra are secondary Bragg peaks caused by multiple scatterings. It is shown in Fig. 3 that longer electron mean free path lowers the peaks and lifts the dips in the spectra.

### 3.2 Phase shift and LEED spectra

In the figure caption of Fig. 4 “Born” denotes the Born approximation for the  $s$ -wave phase shift, where the Thomas-Fermi potential

$$V(r) = -(2Z/r)e^{-z^{1/3}r} \quad (Z: \text{atomic number})$$

was used to describe the scattering potential. A small phase shift corresponds to a small atomic scattering factor. Figure 4 shows that in the spectra calculated with smaller atomic scattering factors the height of peaks, especially those caused by multiple scatterings are lowered. In the case of  $\delta(K)=\pi/2$  the calculated spectra are in good agreement with experimental ones. Thus we adopt  $\delta(K)=\pi/2$  as an approximate value of phase shift.

### 3.3 Angle of incidence and LEED spectra

Figure 5 shows how LEED spectra depend on the angle of incidence

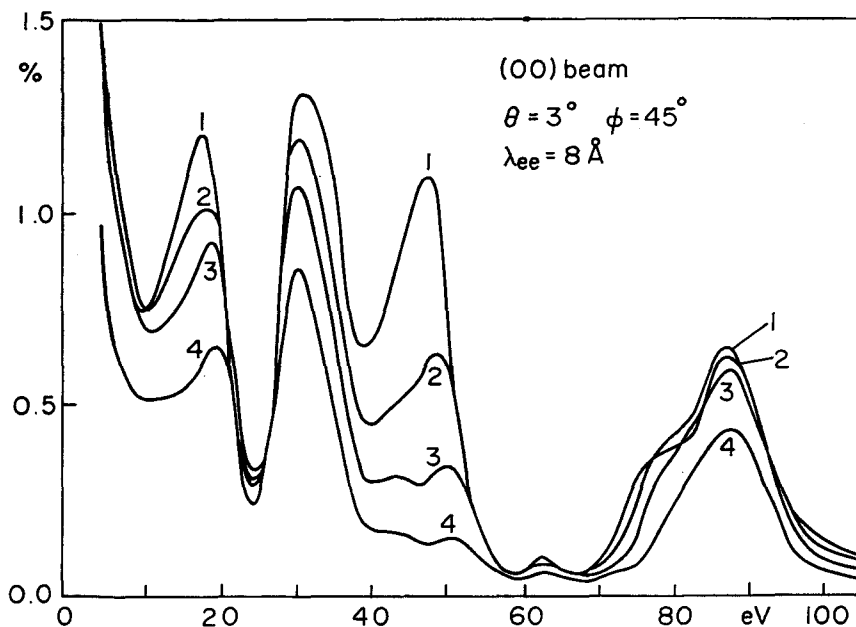


**Fig. 4.** Dependence of LEED spectra on the phase shift.  
 $\delta_s$ : 1)  $\pi/2$ , 2) “Born”, 3)  $\pi/3$ , 4)  $\pi/4$ .

Y. HAMAUZU

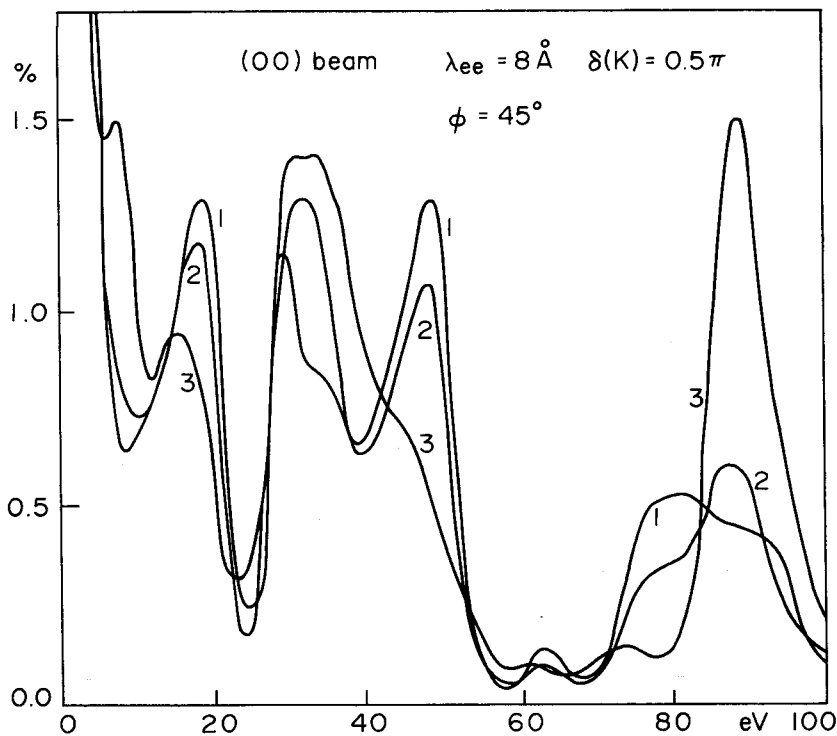


Fig. 5. Dependence of LEED spectra on the angle  $\theta$  of incidence measured from surface normal.  
 $\theta$ : 1)  $0^\circ$ , 2)  $3^\circ$ , 3)  $6^\circ$ .

of the electron measured from the surface normal. The azimuthal angle is  $45^\circ$ , *i.e.*, azimuth is in the  $[11]$  direction.

According to the kinematical theory based on the single scattering events, larger angle of incidence shifts the peak positions to higher energies. Actually the primary Bragg peaks at about 40 and 90 eV behave according to the predictions of the kinematical theory. On the other hand the secondary Bragg peaks at about 20 and 50 eV show the opposite behavior to the primary Bragg peaks. This sort of phenomenon was first observed by McRAE and CALDWELL<sup>20</sup> in the LEED spectra from the LiF (100) surface. After two years McRAE developed a multiple scattering theory of LEED and was able to explain this phenomenon on the basis of his theory.

#### 3.4 Correlation between calculated and experimental LEED spectra

Figures 6, 7, and 8 show LEED spectra of the (00), {10}, and {11} beams, respectively. The parameters used are indicated in the panel.

*An S-Wave Multiple-Scattering Approach to Low-Energy Electron Diffraction*

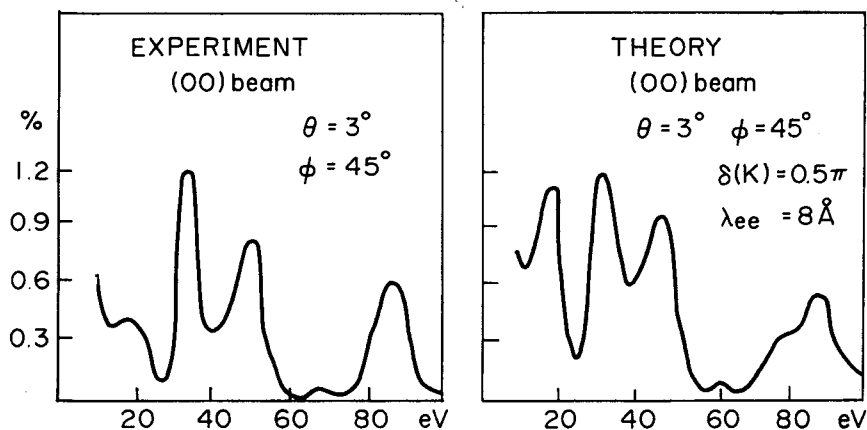


Fig. 6. Comparison between the calculated and experimental LEED spectra for the (00) beam.

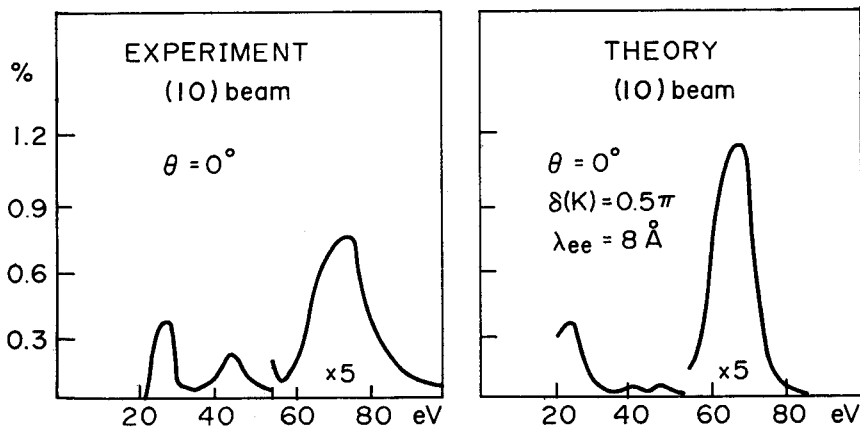


Fig. 7. Comparison between the calculated and experimental LEED spectra for the (10) beam.

Calculated spectra are normalized so that the heights of peaks near 35, 20, and 55 eV in the spectra of the (00), {10}, and {11} beams, respectively, are equal to the heights of the corresponding peaks in Andersson's experiments.

As a whole the calculated positions of peaks are in good agreement with experimental ones. The calculated heights of the peaks in the case of the (00) beam are in fairly good agreement with experiments, whereas those of the secondary Bragg peaks in the case of the {10} and {11} beams

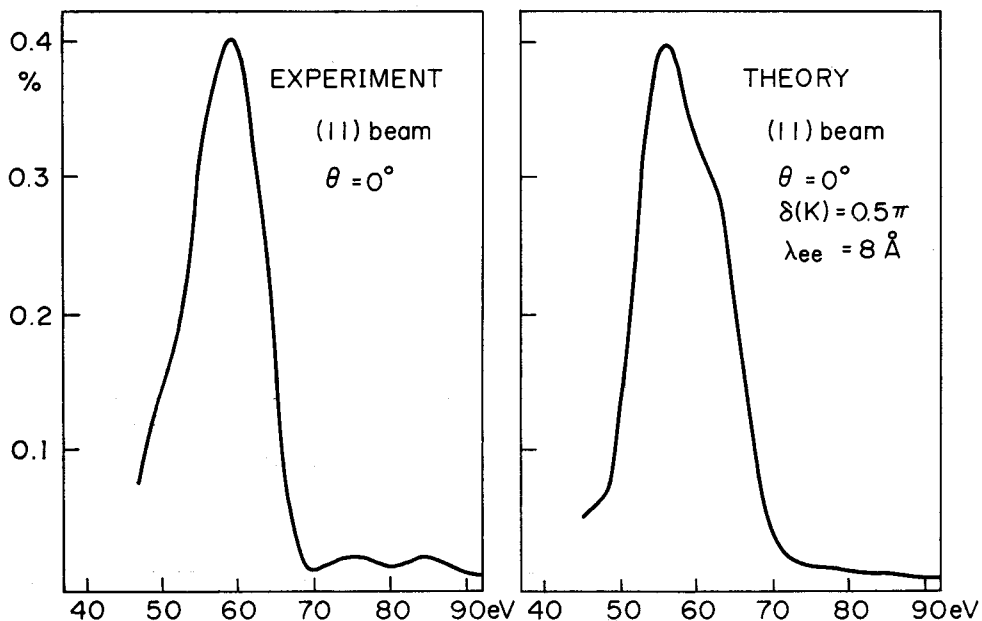


Fig. 8. Comparison between the calculated and experimental LEED spectra for the (11) beam.

are very small as compared with experiments. This indicates that the secondary Bragg peaks depend more on the details of the atomic scattering factor as compared with the case of the primary Bragg peaks.

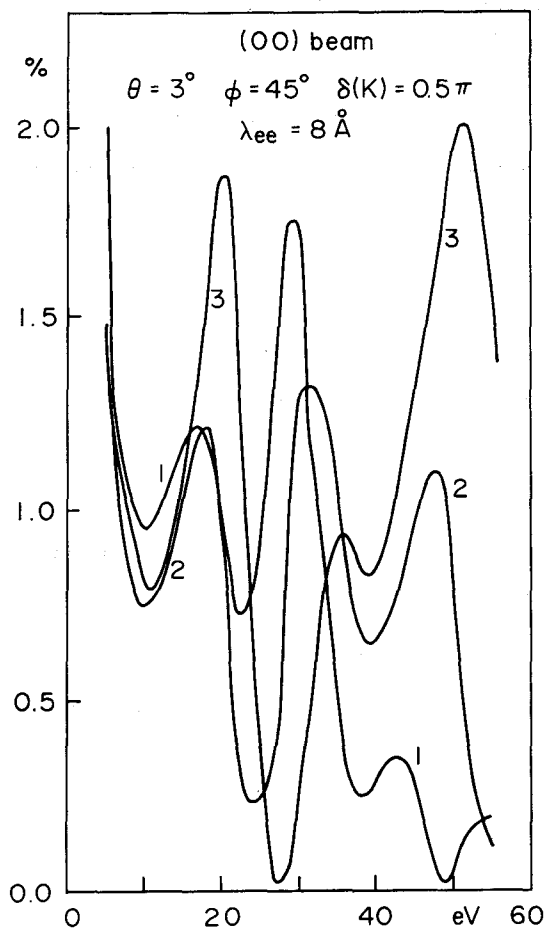
### 3.5 Relaxation or contraction of a surface and LEED spectra

Figure 9 shows the dependence of the LEED spectra of the (00) beam on the relaxation or contraction of a surface. Let us denote the separation between the first and second atom layers and the separation between layers in the bulk crystal by  $d'$  and  $d$ , respectively. Curves 1, 2, and 3 correspond to the spectra from the model surface with  $\alpha=0.1, 0, -0.1$ , respectively, where  $\alpha$  is defined by  $d'=d(1+\alpha)$ . It is found that the spectra from the relaxed or contracted surface is not in good agreement with the experimental one. It is also seen that LEED spectra change critically depending on the relaxation or contraction of the surface.

## § 4. Concluding remarks

A simplified method for calculating LEED spectra has been developed on the basis of the  $s$ -wave approximation. The LEED spectra from the

*An S-Wave Multiple-Scattering Approach to Low-Energy Electron Diffraction*



**Fig. 9.** LEED spectra of the (00) beam from relaxed or contracted surface. The curves 1), 2) and 3) show the spectra for the cases in which the separation of the surface layer contract by 10%, 0% and -10%, respectively, as compared with the bulk value.

copper (100) surface have been calculated by using this method and it has been observed that as a whole calculated peak positions are in good agreement with experiments and the heights of the primary Bragg peaks are also in good agreements, whereas the heights of the secondary Bragg peaks of the non-specular beams are very small as compared with experiments. It has been found that the separation between the first and second atomic layers neither relax nor contract more than 10% of the bulk value.

Y. HAMAUZU

In conclusion the present method based on the *s*-wave approximation is relatively simple and of practical value for analyzing LEED spectra.

### Acknowledgements

The author wishes to express his sincere thanks and appreciation to Prof. T. TOYA for his encouragement in the course of the present work and to Prof. T. NAKAMURA for his critical reading of the manuscript and to Mr. Y. ONO for valuable discussions.

### References

- 1) P. J. ESTRUP and E. G. MCRAE, *Surface Sci.*, **25**, 1 (1971).
- 2) S. ANDERSSON and J. B. PENDRY, *J. Phys. C: Solid state Phys.*, **5**, 141 (1972).
- 3) K. KAMBE, *Z. Naturforsch.*, **22 a**, 322 (1967).
- 4) J. L. BEEBY, *J. Phys. C: Solid State Phys.*, **1**, 82 (1968).
- 5) Y. HAMAUZU, *Phys. Letters*, **43 a**, 191 (1973).
- 6) K. HIRABAYASHI and Y. TAKEISHI, *Surface Sci.*, **4**, 150 (1966).
- 7) D. S. BOUDREAX and V. HEINE, *Surface Sci.*, **7**, 426 (1967).
- 8) Y. H. OHTSUKI, *J. Phys. Soc. Japan*, **24**, 1116 (1968).
- 9) G. CAPART, *Surface Sci.*, **26**, 429 (1971).
- 10) E. G. MCRAE, *Surface Sci.*, **11**, 479 (1968).
- 11) P. M. MARCUS and D. W. JEPSEN, *Phys. Rev. Letters*, **26**, 1365 (1971).
- 12) C. B. DUKE and C. W. TUCKER, JR., *Surface Sci.*, **15**, 231 (1969).
- 13) K. HIRABAYASHI, *J. Phys. Soc. Japan*, **30**, 211 (1971).
- 14) J. C. SLATER, *Phys. Rev.*, **51**, 140 (1937).
- 15) K. KAMBE, *Z. Naturforsch.*, **23 a**, 191 (1968).
- 16) E. G. MCRAE, *J. Chem. Phys.*, **45**, 3258 (1968).
- 17) L. Van HOVE, *Phys. Rev.*, **95**, 249 (1954).
- 18) D. W. JEPSEN, P. M. MARCUS and F. JONA, *Phys. Rev.*, **B 5**, 3933 (1972).
- 19) S. ANDERSSON, *Surface Sci.*, **18**, 325 (1969).
- 20) E. G. MCRAE and C. W. CALDWELL, JR, *Surface Sci.*, **2**, 509 (1964).